Surface and Subsurface Geochemical Monitoring of an EOR-CO2 Field: Buracica, Brazil.

Caroline Clotilde Magnier, Virgile Rouchon, Carlos Bandeira, R. Goncalves, D. Miller, R. Dino

Dossier

Monitoring of CO₂ sequestration and hydrocarbon production
Monitoring pour le stockage du CO₂ et la production des hydrocarbures

Surface and Subsurface Geochemical Monitoring of an EOR-CO$_2$ Field: Buracica, Brazil

C. Magnier[1], V. Rouchon[1], C. Bandeira[2], R. Gonçalves[2], D. Miller[2] and R. Dino[2]

1 IFP Energies nouvelles, 1-4 avenue du Bois-Préau, 92852 Rueil-Malmaison - France
2 PETROBRAS-CENPES/PDEXP, rua Horácio Macedo n.950, Cidade Universitária, Ilha do Fundão, Rio de Janeiro, 21941-915 - Brasil
e-mail: caroline.magnier@ifpen.fr - virgile.rouchon@ifpen.fr - carlosbandeira@petrobras.com.br - rona@petrobras.com.br
miller@petrobras.com.br - dino@petrobras.com.br

Résumé — **Monitoring géochimique en surface et sub-surface d'un gisement en production par récupération assistée et injection de CO$_2$: le champ de Buracica, Brésil** — Le monitoring géochimique du gisement de Buracica, qui produit des hydrocarbures par récupération assistée et injection de dioxyde de carbone, est présenté dans cet article. Une méthodologie permettant de coupler l'utilisation des isotopes stables du carbone et des isotopes des gaz rares pour étudier la faisabilité de traçage d'une fuite de CO$_2$ du réservoir à la surface est détaillée. Les campagnes de prélèvement se sont déroulées sur trois périodes en deux ans, permettant de mesurer la variabilité des teneurs en CO$_2$ dans les sols et dans les réservoirs pétroliers. La distribution du CO$_2$ en surface varie de 0,8 à 14 % et peut être contrôlée en partie par les propriétés des sols et la topographie. Les résultats isotopiques du $\delta^{13}C_{CO_2}$ varient entre –15 et –23 ‰ et suggèrent que le flux de CO$_2$ soit principalement biogénique. Le gaz injecté, puis produit à Buracica, est hétérogène en composition de par la récupération tertiaire du gisement induisant une infiltration de CO$_2$ à des niveaux variables et les variations de perméabilité au sein même du réservoir. Les résultats montrent qu'il est, dans ce cas, difficile de tracer le CO$_2$ du réservoir à la surface en fonction des valeurs isotopiques $\delta^{13}C_{CO_2}$. Notre approche démontre le fort potentiel des gaz rares pour discriminer des mélanges, même à des teneurs faibles de CO$_2$ (~1 %). Les résultats illustrent le potentiel de ces nouvelles techniques de monitoring géochimiques pour suivre le CO$_2$ dans les projets de séquestration combinant les signatures du carbone stable avec celles des gaz rares.

Abstract — *Surface and Subsurface Geochemical Monitoring of an EOR-CO$_2$ Field: Buracica, Brazil* — *This paper presents a surface and subsurface geochemical survey of the Buracica EOR-CO$_2$ field onshore Brazil. We adopted a methodology coupling the stable isotopes of carbon with noble gases to investigate the adequacy of geochemical monitoring to track deep fluid leakage at the surface. Three campaigns of CO$_2$ flux and concentration in soils were performed to understand the CO$_2$ variability across the field. The distribution of the CO$_2$ soil contents between 0.8 and 14% is in great part controlled by the properties of the soil, with a first-order topographic dependency. These results, together with a $\delta^{13}C_{CO_2}$ between –15 and –23‰, suggest that the bulk of the soil CO$_2$ flux is biological. The gas injected and produced at numerous wells across the field showed a great spatial and somewhat temporal heterogeneity with respect to molecular, $\delta^{13}C_{CO_2}$ and noble gas compositions. This heterogeneity is a consequence of the EOR-induced sweeping of the petroleum fluids by the injected CO$_2$, producing a heterogeneous mixing controlled by the production scheme and the distribution in reservoir permeability. In light of the $\delta^{13}C_{CO_2}$ found in the reservoir, the stable isotopic composition of carbon was insufficient to track CO$_2$ leaks at the surface. We demonstrate how noble gases may be powerful leak discriminators, even for CO$_2$ abundances in soils in the bottom range of the biological baseline (~1%). The results presented in this study show the potential of geochemical monitoring techniques, involving stable isotopes and noble gases at the reservoir and soil levels, for tracing CO$_2$ in CCS projects.*

INTRODUCTION

Carbon Capture and Storage (CCS) projects in geological depleted petroleum fields or deep saline aquifers [1-4] have been envisaged as solutions to mitigate increasing atmospheric CO_2. The enhanced recovery of oil (EOR) based on the injection of CO_2 is an expanding technology that offers the advantage of limiting CO_2 emissions in addition to an increased oil production. Furthermore, it provides the opportunity to study the migration of CO_2 in an oil-producing field and to develop site surveillance methodologies as a part of the CCS technology. The storing of acid gases in underground structures, aquifers or depleted reservoirs would involve field operators to guarantee the containment of the gas and public safety at the surface and subsurface levels above storage sites.

In this study, the investigation of an on-shore EOR-CO_2 field was motivated by the opportunity it provided to have a shallow (–500 m) hydrocarbon depleted petroleum field as a CO_2-storage analogue case study. The Buracica field, in Brazil, was chosen by Petrobras to jointly monitor the surface and subsurface of the oil production area, during a period of one year and a half. The field has undergone an enhanced hydrocarbon tertiary process since the mid-1990s, after most hydrocarbons were extracted by conventional production means [5-6]. The CO_2 is transported by a surface pipeline network, from a fertiliser plant located in the state of Bahia.

This paper will present a series of geochemical surveys at the reservoir level and at the surface, and the technical aspects developed, with the objective of delivering a robust geochemical monitoring methodology, adapted to geological gas storage.

Historically, petroleum system studies have inherited a wide use of gas geochemistry to understand the fate of organic matter, during the diagenetic geochemical steps involving hydrocarbon generation and expulsion from the source rocks to their migration in trapping structures. More specifically, a major problem resides in the use of the stable isotopic composition carbon to identify the origin of CO_2, since it may be fractionated by many organic and inorganic reactions while having various potential sources in the crust. Indeed, carbon dioxide is present in the atmosphere, produced and used by all life forms, generated by organic matter decay, and produced from rock diagenesis and metamorphism, and may also degas from the Earth's mantle. The combined approach of carbon isotopes and noble gases has proven to be effective in the tracking of these different origins and processes [7-10]. In our methodology for CO_2-storage monitoring, we used a similar approach.
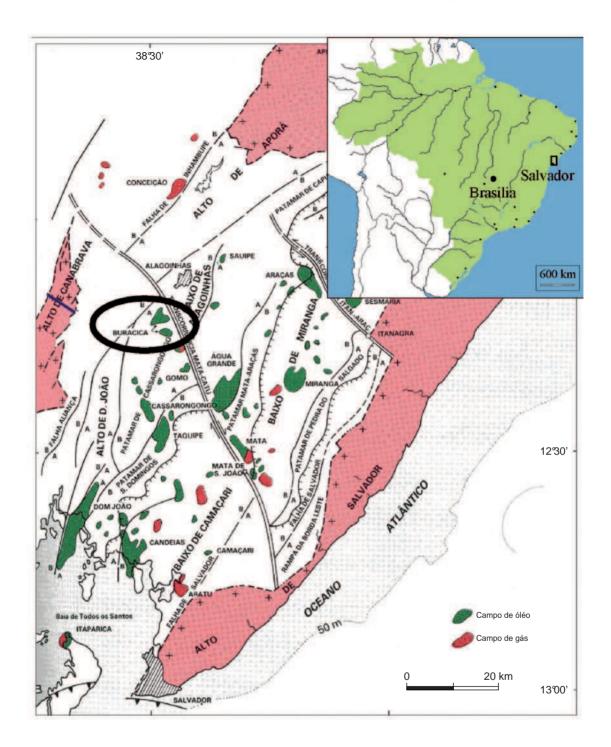
The approach is based on the use of inert tracers, the noble gases, which are always found as trace elements in natural fluids, including CO_2. Whereas major gas compounds, and especially CO_2, may be affected by different bio-chemical processes, the noble gases will only be affected by physical processes (mixing, solubility and diffusive effects). The noble gases will carry the information tied to the processes of fluid migration only, which is the primary concern in the monitoring of CO_2 geological storage sites. The decoupling of the evolution of reactive species and the noble gas during the life of a fluid-rock system is at the centre of the geochemical monitoring methodology presented in this paper. Although fairly well used in the case of natural gas occurrences, this tracing technique has not yet been thoroughly tested on industrial gas storage sites [11-18].

The first objective of the work was to determine the long-term impact of the CO_2 injection at the surface (a few metres) by establishing a repeated survey through the regional mapping of the CO_2 content in soils. The second was to investigate the heterogeneity of the reservoir gas chemistry after a prolonged injection of CO_2. The main challenge in this study resided in developing tools allowing for the discrimination of biogenic and anthropogenic CO_2 at the soil level.
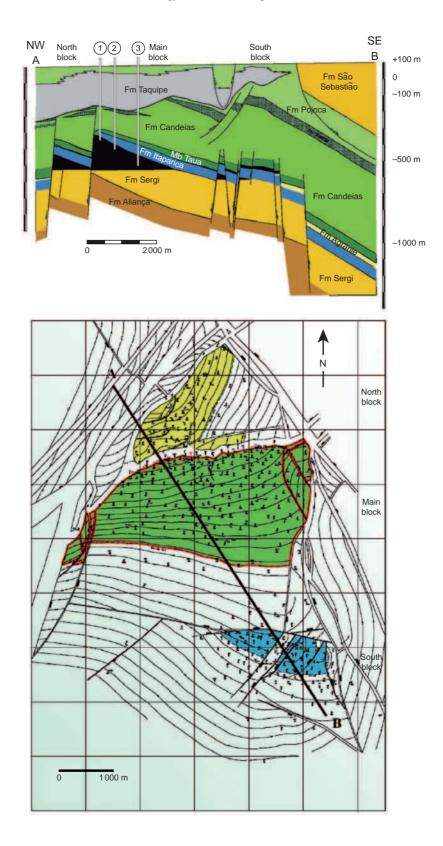
1 AREA OF STUDY

The Recôncavo Basin is located in the state of Bahia in North-Eastern Brazil, about 85 km from the city of Salvador *(Fig. 1)*. It is part of a rift formed between the Late Jurassic era and the Early Cretaceous. The Buracica geological structure, like most neighbouring oil discoveries in this particular geological province, is associated with pre-rift traps that formed by faulted blocks which were set in direct lateral contact with the source rocks of the Candeia Fm [19-20]. The field occupies an area of about 7 km^2 enclosed in a rectangle measuring about 2×4 km *(Fig. 2)*. The exploration of the basin started in the 1930s and hydrocarbon reserves were economically viable from the 1950s to the 1970s. The petroleum system in Buracica resulted from short migration distances of generated hydrocarbons between the source rocks to reservoirs with organic matter-rich cap rocks acting as both regional seals and secondary reservoirs. The main producing reservoirs are positioned in the Sergi-C Formation, and divided into 14 production zones. Sergi-C units predominantly constitute eolic and fluvial facies and are isolated from other reservoirs by a shaly sand barrier. In the Main Block, there is an average dip angle of 6 degrees and units have an average thickness of 9 metres. The reservoirs have an average porosity of about 22% and an average initial water saturation of about 24% with permeability ranging from 150 to 900 millidarcies. Permeability and porosity in the reservoirs have been affected by different diagenetic processes. Two main diagenetic sequences occurred depending on the origin of the sandstones, pre-rift (fluvial/eolian types) or syn-rift (lacustrine deposits). A general decreasing trend of porosity is observed with increasing depth. Reservoir temperature is on average 44ºC, oil gravity averages 35º API and the oil viscosity ranges from 2 to 10 centipoises for the usual range

Figure 1

Location of the Buracica field, within the Recôncavo Basin, Brazil (adapted from [23]). The distribution of the oil and gas fields is shown.

of pressure in reservoir conditions. Measured in relation to the sea level, the depth of the original oil/water contact is –525 metres, and the highest portion of the reservoir has a depth of – 305 metres *(Fig. 2)*.

An immiscible CO$_2$ flooding project was implemented in 1991 in the Sergi-C reservoir (also known as Sergi-1) of the Main Block, allowing an increase in the oil recovery factor from 9.9 to 29.4%. The additional recovery factor is about

Figure 2

Map and cross-section of the Buracica field. Circled labels 1, 2 and 3 in the cross-section correspond to the implantation of CO_2 injector, water injector and oil producer wells, respectively. The map represents the three production blocks of the Buracica field, with in the background the contour lines of the depth of the top of the Sergi Fm and the main faults structuring the reservoir. The main block (green on the map) is where the CO_2 injection and the geochemical survey were performed (adapted from [23]).

9.5% of OOIP; *i.e*., it was expected to recover more than 4.4% of the oil over the pre-injection production [5]. The injection of CO$_2$ was operated by seven aligned wells located in the northern border of the main hydrocarbon-producing block, where the reservoir is the shallowest *(Fig. 2)*. This allowed the reservoirs to maintain a gas cap. Seven water injection wells were implemented at the gas-oil contact in order to limit the breakthrough of the injected gas and to improve the efficiency of the injection [6]. The entire studied area is delimited by a system of structural regional faults to the North and to the East (Mata Catu fault). Major faults are depicted on the contour level maps of the Sergi fm. *(Fig. 2, 3)*.

2 SAMPLING AND MEASUREMENT STRATEGY

2.1 Surface Gas Monitoring and Sampling

A surface baseline is a key feature in a geochemical monitoring programme. It is a prerequisite for the assessment of the natural variability of CO$_2$ in soils in terms of content and isotopic signatures. The soil CO$_2$ content at the surface was compiled from three monitoring surveys at different periods of the year, August 2008, March 2009 and October 2009. The geochemical surveys #1 and #2 took place during a period of injection of CO$_2$ gas in reservoirs for enhanced oil recovery. The last survey was performed after the CO$_2$ injection had ceased and during a phase of N$_2$ injection.

An initial regular grid with thirty surface soil points distanced by approximately 500 metres was deployed over the northern central main block *(Fig. 3)*. Thirty soil sites were sampled in the first two monitoring campaigns, and that number doubled in the last monitoring survey in October 2009 because of the availability of more analytical equipment. Additional points were chosen near the east of the field and in the northern block, beyond the main production block. In the latter, the goal was to check the CO$_2$ content above reservoirs where no CO$_2$ was ever injected.

2.2 Reservoir Gas Sampling

The subsurface reservoirs were sampled during every field survey for:
– the CO$_2$ source prior to injection at a satellite station and at two injector wells, and;
– hydrocarbon producing wells in the Sergi C and less commonly in the Agua Grande geological formations.

Two additional wells were sampled in October 2009 in the northern block in order to have a record of the natural reservoir composition there, as the area is unaffected by EOR-CO$_2$ injection. Figure 3 shows the location of the wells sampled.

The gas sampling was performed directly at the well heads. Because not all wells were producing at the time of sampling, a flushing time was allowed for the well to release the accumulated fluids, which might have been affected by contaminating processes. Before sampling, a portable CO$_2$, H$_2$S and hydrocarbon gas analyser was placed in the flow of the purged well in order to follow the stabilisation of the gas composition and to ensure a sufficient purge of the well. After stabilisation, a sampling line was connected to an oil/gas/water separator and pressure regulators to fill the stainless steel gas tubes with a limited amount of liquids, and to ensure a low gas pressure of 2 bar.
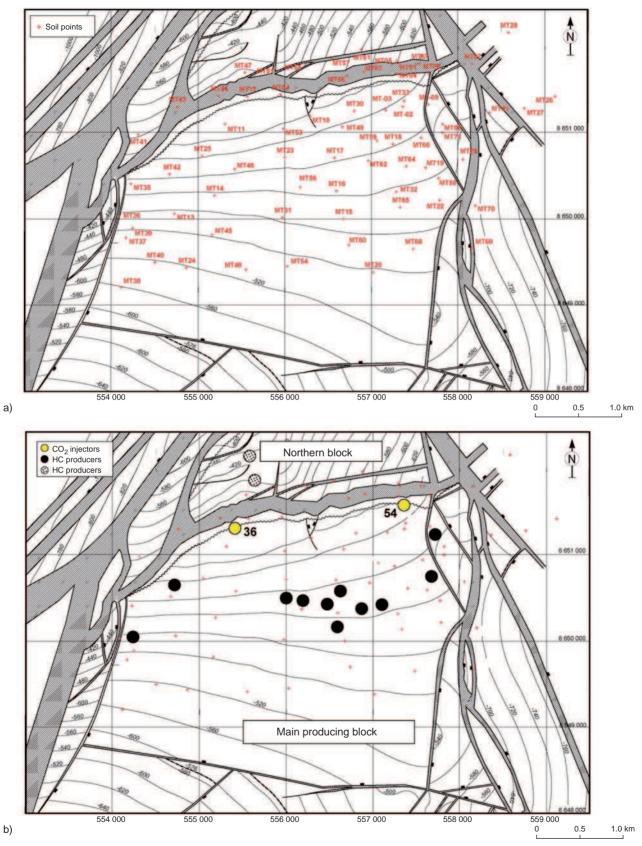
2.3 Analytical Procedures

2.3.1 Flux Measurements

The flux of CO$_2$ emanating at the surface was measured using a West System flux chamber with a LICOR LI-820 carbon dioxide detector. The chamber allows a gas flux to accumulate in a fixed and constant volume, where CO$_2$ (possibly including CH$_4$ or H$_2$S) abundances are monitored during a user-defined time span (typically here 300 seconds). The slope of the abundance *versus* time trend gives the average flux during this time span. At each soil monitoring point, two to four flux measurements were made several metres apart in order to define a representative average of the local flux, as much as possible, independent of small-scale soil heterogeneities. Additional flux measurements were made just above the 1-m-deep holes used for direct soil gas sampling in order to estimate the effects of the hole on the degassing of CO$_2$.

2.3.2 Direct Measurement of Soil Gases

For field analyses, the soil gas is pumped through a stainless steel probe inserted in the ground at a depth of 1 metre. The sampling head of the probe is connected to a 1/8th-inch tubing, itself connected to an instrument for analysis. The soil gas compositions of CO$_2$, O$_2$, N$_2$, CH$_4$, and traces of C$_2^+$ hydrocarbons were determined by a VARIAN micro-gas chromatograph CP4900. Alternately, a GA2000+, an Orion+ and a metrex portable instrument were used to quantify CO$_2$, methane and oxygen in the soil gas.

Soil gases were sampled in glass Vacutainers® or stainless steel tubes and brought back to the laboratory for carbon isotopic and noble gas analyses (see appendix for details of the analytical procedures). The procedure to collect soil gas aims at minimising the air contamination of the sample. The sampling loop has a volume of 10 cm^3 which is vacuumed prior to sampling with a manual pump, through which a stainless steel sampler isolated by pressure valves and a Vacutainer can be filled. The sampling loop is connected to the gas probe introduced into the soil at one metre depth. The soil gas is admitted to the sampling tube through the sampling loop and the gas probe by pressure difference, and is left to equilibrate from the tube to the soil for 5 minutes.

Figure 3

Location of the survey soil points a) and wells b) superimposed on the structural maps of the top of the Sergi Fm.

During the last field survey, two points showing the highest CO_2 contents were investigated in depth by drilling holes down to 5 metres below the surface. A sampler isolated by a packer was developed in order to collect gas in deeper soil horizons with minimum atmospheric air contamination from the borehole itself. Immediately after digging one metre of soil, the packer was introduced and inflated in order to let the soil gas equilibrate with the sampler, after which the soil gas was sampled and analysed at the surface. This operation was repeated five times down to 5 metres.

3 RESULTS AND DISCUSSION

3.1 Surface Monitoring

3.1.1 Surface Monitoring Data

Flux measurements were performed only in the first and second surveys. The first period of monitoring was characterised by an average CO_2 flux of 0.37 moles/m²/day with an overall standard deviation of 0.45 moles/m²/day. Minimal and maximal values were 0.07 and 2.1 moles/m²/day, respectively. The second period was characterised by an average CO_2 flux of 0.20 moles/m²/day with an overall standard deviation of 0.21 moles/m²/day. Minimal and maximal values are 0.07 and 0.48 moles/m²/day, respectively. A 25-metre flux measurement grid was also made around the highest enriched soil site where a high CO_2 concentration was found in all three fieldwork campaigns. This limited area was characterised by great flux heterogeneity with minimum and maximum values of 0.04 and 1.35 moles/m²/day, respectively.

The CO_2 content in soils is summarised for the three monitoring surveys in Figure 4. Soils showed a wide range of CO_2 concentrations as expected because of natural heterogeneities. The CO_2 content varied between 0.8 and 14% in the first survey (August 2008), with a majority of points between 4-9%. During the second survey (March 2009), the CO_2 concentrations were on average lower, with values fluctuating between 0.9 and 6.2%. In the third monitoring period (October 2009), soil gases showed CO_2 contents from 0.8 to 8%.

The additional measurements of soil CO_2 at points 3 and 42 in the last survey show a consistent increase in CO_2 contents with depth down to –5 metres, with up to 20 and 9.8% at each point, respectively *(Tab. 1)*.

3.1.2 Surface Monitoring Discussion

A strong spatial and temporal variability in the CO_2 concentration in soils was witnessed above the Buracica field *(Fig. 3)*. The CO_2 content in soils plotted against the altitude of the measurement point shows a rough reverse correlation *(Fig. 5)*, which is repeated for each survey, although with a variable amplitude. The Buracica area can be described as rolling hills with

TABLE 1

Stable carbon isotope data from a reduced selection of soils

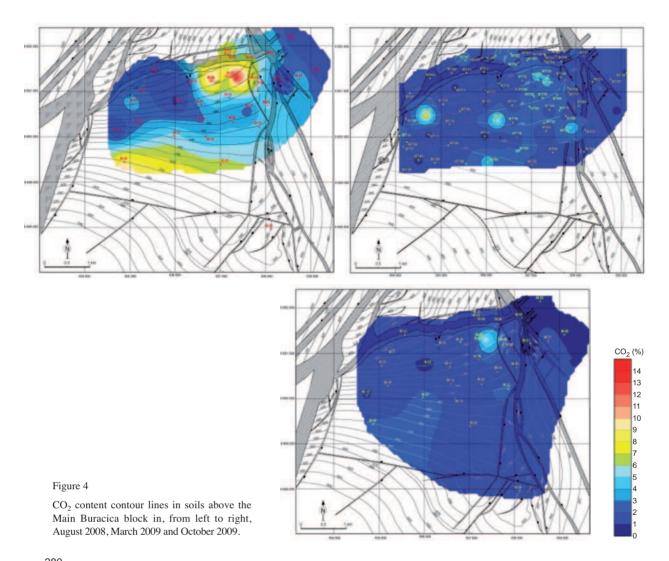| Soil point	Altitude	Depth (m)	% CO_2	$\delta^{13}C$ (‰)
M-02	188	0.8	14.4	-14.6
MR-02	188	1.0	6.5	-19.7
MR-02	188	2.0	6.0	-19.6
MR-02	188	3.0	8.5	-20.4
MT3	197	4.0	13.5	-22.9
MT3	197	5.0	20.2	-24.1
MR-09	190	1.0	3.2	-21.9
MR-09	190	3.0	2.5	-22.4
M-30	210	0.8	12.7	-15.8
MR-34	193	1.0	1.5	-19.2
MT-42	177	4.0	9.8	-18.0

M-Survey 1 (August 2008).
MR-Survey 2 (August 2009).
MT-Survey 3 (March 2009).

meadows at altitudes of 150 metres and hills culminating at 220 metres *(Fig. 6)*. Although not measured in this survey, the organic matter and clay content in soils is known to be inversely correlated with altitude in rather uniform soil-substratum lithological contexts [21-22]. A high abundance both in organic matter and in clay is a factor favouring the biological activity. In such soils, the nutrients necessary for the growth of plants and the organic matter required for soil respiration are available and enriched, compared with organic-poor sandy soils, for example. This systematic correlated distribution of soil nature and CO_2 contents indicates that the first-order CO_2 origin and variability is tied to biology within the soil, and can be interpreted to be representative of the natural background. Two points (02 and 03) seemed to be outside the general rule, as they were characterised by consistently high CO_2 contents at a topographical high in each survey.

The carbon isotopes were evaluated on only a handful of soil gas samples *(Tab. 1)*. The CO_2 carbon isotopic $^{13}C/^{12}C$ data from selected soils with variable CO_2 content obtained during the various monitoring surveys show the CO_2 gas in soils to have relatively heterogeneous carbon isotope ratios ranging between –15 and –24‰. This range of carbon isotopic ratios is fully consistent with a biological soil origin, although not exclusively [23].

The soil CO_2 fluxes are not correlated with the CO_2 contents in the soil, unless plotting the average values for each survey *(Fig. 7)*. No correlation could be made in order to justify the observed distribution of flux data. Whereas the amount of CO_2 in soils seems correlated with parameters governed by the topography, we suggest that the fluxes are related to the physical characteristics of the soil. Indeed, the upwelling flux of the CO_2 produced in situ will depend on the permeability

Figure 4

CO_2 content contour lines in soils above the Main Buracica block in, from left to right, August 2008, March 2009 and October 2009.
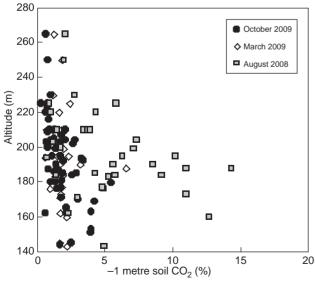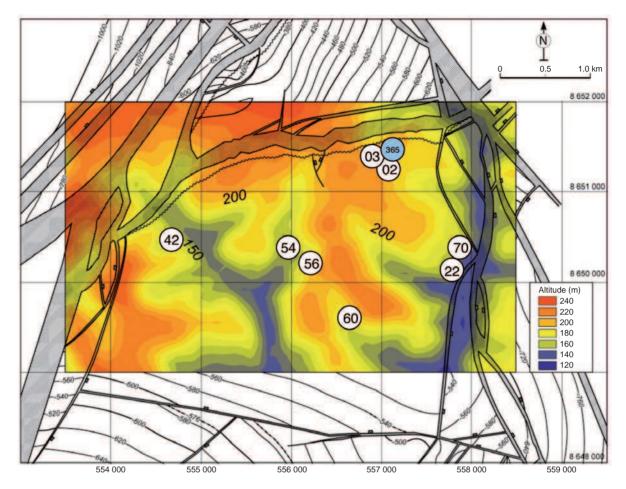

Figure 5

Distribution of the soil CO_2 concentrations with altitude for the three surveys.

and tortuosity of the soil, which are tied to the texture and water saturation of the soil [24-25]. However, given the lack of constraints on meteorological and petrophysical variables as well as the water saturation, it is impossible at the moment to interpret flux data.

3.2 Subsurface Reservoir Monitoring

3.2.1 Composition and Carbon Stable Isotopes

The CO_2 injected from the satellite station through the CO_2 injector wells 36 and 54 of the Buracica main block was sampled for each survey *(Fig. 3)*. The proportion of CO_2 is above 98% and nitrogen, methane and traces of hydrogen make up the rest of the gas composition *(Tab. 2)*. It is difficult to differentiate the injected CO_2 in wells 36 and 54 from relative composition and isotopic data. The carbon isotopic ratios for the injected CO_2 range from –30.9 to –32.6‰

Figure 6

Location of several soil points of interest in the topographic contour lines above the Buracica field. Soil points 3 and 42 were targeted for further investigations given their high CO$_2$ concentrations *(Fig. 4)*.

Figure 7

Distribution of soil data in a CO$_2$ flux *versus* CO$_2$ concentration diagram.

TABLE 2

Composition and carbon isotope data of CO$_2$ source and CO$_2$ injector wells

Monitoring survey	Source or CO$_2$ injector	CO$_2$ % Composition	$\delta^{13}C_{CO_2}$ Isotopes
Survey 1	Satellite CO$_2$	99.0	-32.6
Survey 2	Satellite CO$_2$	99.0	-30.9
Survey 3	Satellite CO$_2$	99.1	-31.0
Survey 1	Well 54 CO$_2$ injector	97.9	-32.7
Survey 3	Well 54 CO$_2$ injector	98.5	-33.8
Survey 1	Well 36 CO$_2$ injector	97.8	-32.2
Survey 2	Well 36 CO$_2$ injector	98.7	-31.7

and little difference was observed between the satellite station and the injector wells throughout the different surveys.

Reservoir gases issued from the Sergi and Agua Grande fm. are dominated by CO$_2$, generally at a proportion greater

TABLE 3

Subsurface gas composition and carbon isotopes

Monitoring survey	Well	Geological formation	Normalised (%)							Carbon isotopes (relative to PDB)						Reservoir data		
			%C1	%C2	%C3	%iC4	%nC4	%CO$_2$	%N$_2$*	δ^{13}C C1	δ^{13}C C2	δ^{13}C C3	δ^{13}C iC4	δ^{13}C nC4	δ^{13}C CO$_2$	BSW	HC	H$_2$O
			Gas Chromatography Varian 3800							Mat Finnigan 253 Gcirms (precision of δ^{13}C ± 0.5 per mil)						m^3/day		
Survey 1	Well 1		1.7	0.1	0.5	0.2	0.4	94.9	2.1	-45.2	ND	ND	ND	ND	-33.2			
Survey 2	Well 1		1.6	0.2	0.7	0.3	0.6	93.7	2.9	-45.7		-27.6	-28.8	-26.7	-33.0			
Survey 3	Well 1	SG I-III	0.9	0.3	1.3	0.6	0.9	94.4	1.6	-49.1	-32.3	-28.2	-28.1	-26.6	-34.2	96	5.6	134
Survey 1	Well 2		5.8	0.6	1.4	0.4	0.6	89.3	1.9	-51.1	-31.9	-27.4	-28.8	-26.3	-33.0			
Survey 2	Well 2		3.7	0.7	2.4	1.0	1.4	89.5	1.3	-51.8	-32.3	-27.7	-29.3	-26.5	-33.9			
Survey 3	Well 2	SG I	2.5	0.9	5.7	2.7	4.4	83.6	0.2	-52.0	-32.0	-28.6	-29.2	-26.8	-35.3	87	9.1	61.2
Survey 1	Well 3		7.2	1.4	3.6	1.5	2.7	79.1	4.6	-46.4	-30.4	-26.9	-28.6	-26.6	-31.2			
Survey 2	Well 3		2.6	0.9	3.5	1.3	1.8	89.0	0.9	-47.0	-32.3	-27.7	-29.0	-26.6	-33.5			
Survey 3	Well 3	SG I	2.5	1.0	4.2	1.5	2.0	87.8	1.0	-47.0	-32.6	-28.1	-28.9	-26.7	-34.0	38	35.5	21.9
Survey 1	Well 4		31.3	2.3	3.5	0.9	1.3	52.4	8.4	-46.9	-31.7	-27.6	-28.8	-26.4	-33.4			
Survey 3	Well 4	SG I-III	8.3	1.7	4.4	1.5	2.2	80.6	1.3	-51.4	-32.3	-28.2	-29.2	-26.8	-32.4	94	8.9	147.9
Survey 1	Well 5		81.7	1.0	3.3	1.4	2.4	2.9	7.2	-48.8	-32.2	-27.5	-26.3	-26.5	6.2			
Survey 2	Well 5		67.4	4.4	9.4	2.6	3.2	7.6	5.4	-52.2	-32.1	-27.5	-28.9	-26.5	-3.5			
Survey 3	Well 5	SG I-III	73.2	3.7	7.5	2.1	2.6	6.0	5.0	-50.9	-32.6	-28.2	-29.1	-26.7	-2.1	97	5.3	172.4
Survey 1	Well 6		18.0	0.9	3.0	1.1	1.8	47.9	27.3	-50.2	-28.3	-26.3	-26.7	-25.5	-31.0			
Survey 2	Well 7		2.1	1.0	2.9	1.2	1.7	89.6	1.6	-50.8	-31.8	-27.5	-29.1	-26.3	-33.5			
Survey 3	Well 7	AG-SG I-III	39.1	9.0	14.2	3.9	5.1	23.6	5.0	-52.4	-31.9	-27.9	-29.1	-26.3	-24.5	93	4.3	57
Survey 2	Well 8		54.8	7.2	6.7	1.1	1.7	28.7	0	-59.9	-32.4	-27.8	-27.4	-26.2	-11.0			
Survey 3	Well 9	SG I	0.1	0.1	0.6	0.3	0.7	93.9	4.3	-35.2	-30.8	-29.8	-29.8	-27.8	-36.4	90.5	12.2	131
Survey 3	Well 10	CI SG I-III	49.2	4.9	8.7	2.6	3.7	10.2	20.6	-52.5	-32.8	-28.3	-29.0	-26.8	-25.0	99	1.6	156.6
Survey 3	Well 11	SG I	0.6	0	0.2	0.1	0.2	98.7	0.2	-40.4	ND	-28.5	-29.6	-27.0	-33.5			
Survey 3	Well 12 north	SG I	32.6	6.6	29.4	10.3	13.7	3.4	4.1	-59.6	-32.1	-27.4	-28.8	-26.4	-15.4	98.5	3.8	210.5
Survey 3	Well 13 north	AG	25.1	4.0	17.7	7.7	11.5	20.0	14.1	-58.8	-33.5	-28.4	-28.4	-27.3	-8.6	74	6.4	18.4

* N$_2$ separate from air.

than 80% *(Tab. 3)*. All reservoirs show traces of C1-C4 hydrocarbons in varying proportions. Nitrogen is also present in the reservoir gas. However, the CO$_2$ content was found to be less than 20% at four wells: wells (5, 7, 8 and 10) in the main producing block and two wells in the northern block (12 and 13). Well 7 is unusual, as it was sampled initially in the Sergi fm. and was analysed with 89.6% CO$_2$ and carbon ratios equal to –33‰, like the average injected CO$_2$. Six months later, in October, the Sergi Fm. production units were co-mingled with the Agua Grande fm. and the gas from well 7 then contained 23.6% CO$_2$ with a δ^{13}C of –24.6‰. Carbon isotope signatures from well 5 vary as a function of time, together with an increase in CO$_2$ content from the onset of the field monitoring up until the last survey. Initially, the well gas had a δ^{13}C of CO$_2$ at +6‰ evolving to –4‰ in the last survey *(Tab. 3)*.

The δ^{13}C ratios in the northern block reservoirs have comparatively isotopically heavy CO$_2$, as shown in well 12

with a δ^{13}C value of –15.4‰ (3.4% of CO$_2$) and δ^{13}C of –8.4‰ in well 13 (20% of CO$_2$).

3.2.2 Noble Gases

The injected CO$_2$ (CO$_{2i}$) shows a slightly variable noble gas composition from one survey to another *(Tab. 4)*. The average composition of Helium (He) is 0.4 ± 0.5 ppm, Neon (Ne) is 0.17 ± 0.17 ppm, Argon (Ar) is 224 ± 87 ppm and Krypton (Kr) is 0.79 ± 0.23 ppm. The isotopic composition of Ar displays an average ^{40}Ar/^{36}Ar ratio of 350 ± 10, while He has ^{3}He/^{4}He ratios of 7.8×10^{-8} ± 3.7×10^{-8}. This composition is highly exotic compared with other natural fluid reservoirs of the Earth's system such as the air, the crust, or the mantle. The gas collected at the producing wells was highly heterogeneous in composition, with noble gas heterogeneities roughly following that of the hydrocarbon/CO$_2$ distribution *(Tab. 3)*. Gases containing a major proportion of CO$_2$ (higher than 80%) have noble gas compositions very comparable
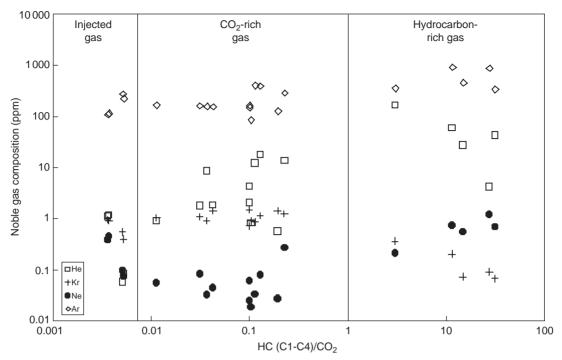
TABLE 4

Noble gas composition of injected fluid, reservoirs and selected soils

		^{4}He (ppm)	+/-	^{20}Ne (ppm)	+/-	^{40}Ar (ppm)	+/-	^{84}Kr (ppm)	+/-	^{40}Ar/^{36}Ar	+/-	^{3}He/^{4}He	+/-
Survey 1	Well 54 CO$_2$ inj	1.21	0.09	0.455	0.420	117.0	14.6	0.909	0.108	336.8	15.6	7.55E-07	2.27E-07
	Well 36 CO$_2$ inj	1.14	0.08	0.396	0.036	112.0	14.0	0.966	0.115	337.6	15.6	8.07E-07	4.25E-08
	Well 1	1.81	0.13	0.085	0.009	166.2	20.7	1.101	0.131	373.3	15.7	4.87E-07	1.41E-08
	Well 2	2.09	0.52	0.061	0.022	168.2	30.0	1.514	0.198	367.1	22.0	1.18E-07	5.75E-09
	Well 5	42.80	10.00	0.706	0.123	344.8	61.5	0.068	0.012	305.0	21.9	1.94E-07	9.96E-09
Survey 2	Source	0.01	0.00	0.018	0.006	295.5	14.5	0.790	0.055	363.0	1.1	n.a.	n.a.
	Source	0.15	0.02	0.092	0.010	333.7	17.1	0.850	0.012	354.3	0.8	n.a.	n.a.
	Well 54 CO$_2$ inj	0.09	0.01	0.075	0.007	230.0	11.2	0.400	0.030	351.0	0.9	n.a.	n.a.
	Well 36 CO$_2$ inj	0.06	0.01	0.097	0.010	282.5	14.5	0.554	0.008	354.0	0.8	n.a.	n.a.
	Well 5	60.10	5.10	0.753	0.072	940.4	46.3	0.204	0.014	306.1	0.9	n.a.	n.a.
	Well 2	0.83	0.07	0.019	0.005	87.2	4.3	0.900	0.060	355.4	0.9	n.a.	n.a.
	Well 3	12.30	1.04	0.034	0.044	413.0	21.0	0.860	0.060	334.2	0.9	n.a.	n.a.
Survey 3	Well 54 CO$_2$ inj	0.17	0.02	0.067	0.010	202.6	11.8	1.065	0.069	359.3	3.1	n.a.	n.a.
	Well 3	17.93	1.49	0.081	0.024	402.3	24.9	1.143	0.120	373.2	3.5	n.a.	n.a.
	Well 2	0.58	0.05	0.028	0.008	130.3	8.1	1.421	0.149	326.2	3.0	n.a.	n.a.
	Well 7	166.68	13.85	0.216	0.064	361.7	22.4	0.363	0.038	372.0	3.5	n.a.	n.a.
	Well 10	496.28	44.74	0.615	0.096	1151.6	67.2	0.101	0.007	329.3	2.9	n.a.	n.a.
	Well 12	4.28	0.38	1.230	0.173	905.2	52.8	0.092	0.006	300.9	2.6	n.a.	n.a.
	Well 11	0.92	0.08	0.056	0.009	170.4	9.9	1.043	0.068	378.4	3.3	n.a.	n.a.
	Well 4	14.00	1.16	0.276	0.082	293.5	18.2	1.243	0.131	384.9	3.6	n.a.	n.a.
	Well 1	1.85	0.36	0.045	0.022	158.3	9.8	1.421	0.149	320.6	3.0	n.a.	n.a.
	Well 13	11.00	1.33	17.210	3.303	9753.3	577.7	0.729	0.051	295.7	2.6	n.a.	n.a.
	Well 5	27.56	3.20	0.554	0.109	468.6	27.8	0.074	0.005	292.6	2.5	n.a.	n.a.
Soil gas samples	Point 42 -4m	5.67	0.51	21.533	3.041	9689.2	568.0	0.654	0.043	293.4	2.7	n.a.	n.a.
	Point 3 -5m	4.66	0.42	15.535	2.198	8776.1	511.9	0.597	0.039	292.1	2.5	n.a.	n.a.
	Point 3 -4m	5.20	0.47	15.787	2.233	8487.6	495.1	0.556	0.036	290.6	2.5	n.a.	n.a.
	Point 2 -1m	4.80	0.40	18.700	1.600	9000.0	441.0	0.630	0.040	293.3	0.9	n.a.	n.a.

with that of the CO$_{2i}$ *(Fig. 8)*. Produced gases with a dominant hydrocarbon proportion are characterised by noble gas compositions more typical of natural petroleum systems, with high He (from 10 to 500 ppm) and low Kr content (down to 0.07 ppm), while sharing Ne and Ar contents close to that of the CO$_{2i}$. The isotopic composition of Ar is characterised by ^{40}Ar/^{36}Ar ratios down to 300 *(Tab. 4)*. The He isotopic composition measured for several samples of the first survey displays a ^{3}He/^{4}He of $1.2 \times 10^{-7} \pm 0.05 \times 10^{-7}$.

3.2.3 Reservoir Monitoring Discussion

The EOR process is aimed at maintaining a pressurised gas cap at the top of the main reservoir block through the injection of CO$_2$, with water injection immediately below, which will act as an impermeable barrier creating a piston effect on the oil zone [5-6]. Given the fact that Buracica produces over 90% of water, the produced water is also re-injected at the bottom of the reservoir. As seen in our data, the CO$_2$ breakthrough is widespread in the main block *(Tab. 3; Fig. 9)*, well below the upper water injection front. In the end, only a few wells are spared from the migration of the injected gas, which probably correspond to small compartmentalised blocks within the main block (*e.g.* well 5). The very high (>80%) to intermediate (20-80%) abundances of CO$_2$ in the produced gas indicate that an extensive sweeping of the hydrocarbons has already occurred due to the 17 years of CO$_2$ injection, and that the fluids remaining from the original petroleum field are extremely depleted. It remains unclear if in the present EOR scheme, the CO$_2$ reaches the production wells directly as a gas phase, or if it is solubilised in the formation and injected water, which in term reaches the production wells through advective transport in the reservoir. The small decrease in Ne with decreasing CO$_2$ contents *(Fig. 8)* tends to indicate that the CO$_2$ and the injected noble gases travel in a solubilised form from the gas cap to the production wells, reflecting the high solubility difference between Ne

Figure 8

Evolution of the noble gas composition of the injected and reservoir gas with the ratio of hydrocarbons over CO_2. Three types of gases are differentiated with respect to this ratio.

and CO_2. However, the long period of injection renders such a reasoning complex to apply without a robust flow simulation of the reservoir, and tracking of the noble gas signature of the injected gas throughout the 17 years of injection.
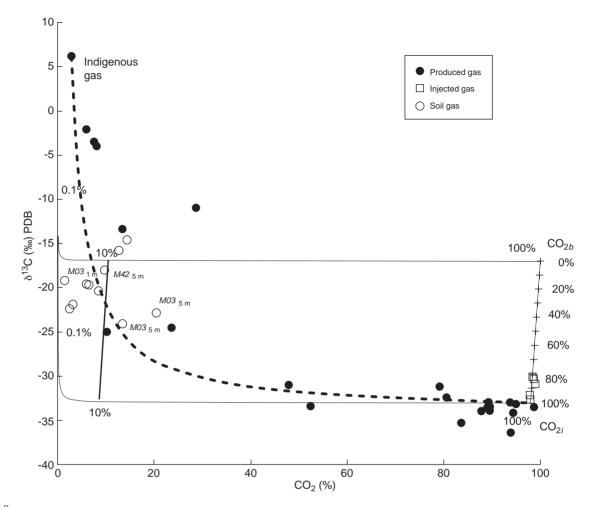
The main conclusion that we can draw from this reservoir survey is that the fluids in the main block are very heterogeneous in composition with respect to CO_2. The heterogeneity is controlled by the flow path of the CO_2, which produces various mixing ratios between the injected CO_2 and the petroleum reservoir gas *(Fig. 8, 9)*. The main concern regarding the surveillance of the field is the gas cap, because it has the greatest potential to leak to the surface. One may not, however, reject the possibility that fluids below the gas cap may leak, and their compositions should therefore be known at all times during any surveillance.

Now, addressing the issue of gas leak tracing, we would like to focus on the carbon isotopic composition of the CO_2 in the reservoir fluids. When plotting the CO_2 content *versus* the carbon isotopic composition of the CO_2 carbon for reservoir gases, we can see how heterogeneous a leaking fluid may be *(Fig. 8)*. Comparing this heterogeneity with the composition in soils, one can see the overlapping of the distributions of both reservoir and soil gases *(Fig. 8)* at low (<10%) CO_2 content. This implies that the carbon isotopic

composition of the CO_2 itself will remain ambiguous for a leak identification at the soil level. Even considering that leaks would be preferentially from the gas cap, which shows a comfortable isotopic difference with soils, one cannot distinguish unambiguously a small contribution of injected CO_2 within biogenic CO_2 in soil gas, given the high background soil CO_2 levels *(Fig. 4)*. When looking at noble gases, we can choose from the set of elements which will give the most discriminating criteria between reservoir and soil *(Fig. 9)*. In Buracica, the injected CO_2 is characterised by

TABLE 5

End-member compositions used for the mixing curves calculated in Figures 8, 10 and 11

	Injected gas	Soil respired CO_2	Produced gas	Air
CO_2 (%)	97.8	100.0	3.0	0.03
C1-C4	-	-	90.0	-
N_2	2.0	-	7.0	80.0
^{4}He (ppm)	1.1	-	42.8	5.2
^{40}Ar	110	-	344	9 300
^{84}Kr	0.90	-	0.07	0.65
δ^{13}C (‰)$_{PDB}$	-31	-17.0	+6.0	-7.0

Figure 9

Distribution of the soil data points in a $\delta^{13}C$ *versus* CO_2 concentration diagram. Various mixing curves are represented. Dashed bold curve: mixing between petroleum gas and the injected CO_2. Crossed solid line: mixing between biological soil CO_2 and the injected gas. Upper thin solid curve: mixing between "heavy" biological soil CO_2 and air (end-member compositions given in Table 5). Bottom thin solid curve: mixing between the injected gas and the air. The percentages indicated on each solid curve represent the mixing proportion of the isotopically lighter end-member. The data for the borehole soil points 03 and 42 are labelled. See text for details.

a high Kr content and a low Ar content compared with the air *(Fig. 9; Tab. 4)*. This Kr content is also much higher than that found in the hydrocarbon-rich reservoir fluids. The He/Kr and the Ar/Kr ratios are therefore good *a priori* discriminators of deep *versus* surface fluids *(Fig. 10, 11)*.

3.3 A Tentative Methodology for Gas Storage Site Surveillance

In order for a valid identification of a deep fluid leakage at the surface to be performed, the conditions of application and the detection limit of any method should be determined. Ideally, a complete monitoring strategy should gather a sufficient number of methodologies to cover all possible leak scenarios. In this geochemical case study, we would like to

emphasise the complementary use of noble gases and carbon isotopes with respect to leak identification at the soil level.

3.3.1 Carbon Isotopes of CO$_2$

Figure 9 represents all analysed data from soils and wells at the Buracica field in a CO_2 *versus* $\delta^{13}C$ graph. We calculated the range of compositions in a ternary mixing system of:

– the injected CO_2;
– the heavy biogenic soil CO_2 (CO_{2b}), and;
– the atmosphere (air), which contains all but two (the heaviest) soil data points from –1 m down to –5 m.

This means that all of the soil gas samples analysed may be interpreted as a mixing of air + CO_{2i} + CO_{2b}, in various proportions, with air contributions in the range 80-99 vol.%.

Figure 10

Plot of the ^{40}Ar over ^{84}Kr ratio *versus* the CO_2 content in injected, reservoir and soil gases. The same mixing curves as in Figure 7 are shown. The dashed envelopes around the solid curves represent a ±2% offset, as an indication of the impact of the analytical uncertainty on the discrimination capabilities of the method.

The CO_2 could either be 100% biogenic with contributions of heavy (–17‰) and light (–30‰) *in situ* soil CO_2 fluxes, or a mixture of heavy CO_{2b} with a minimum of 50% CO_{2i}. However, carbon isotopes alone may not distinguish any of these mixing scenarios. Furthermore, the mixing of the petroleum reservoir gas with the CO_{2i} may produce compositions identical to those found in soils.

3.3.2 Noble Gases

In order to discriminate among various CO_2 end-members, we used the ratios of Ar/Kr and He/Kr in similar graphs *versus* the percentage of CO_2. In the Ar/Kr graph *(Fig. 10)*, no overlapping occurs between the mixing of the petroleum gas with the injected CO_2 and the background soil gas (air). Furthermore, the mixing of the biogenic CO_2 with the

injected CO_2 defines independent compositional trends. In the He/Kr graph *(Fig. 11)*, the discrimination of a CO_2 reservoir fluid from a biogenic soil CO_2 is difficult because of the overlapping of the air noble gas ratio value with the possible mixing between the petroleum reservoir gas and the injected CO_2. However, a leak from the CO_2-depleted parts of the reservoir (*e.g.* petroleum gas) would be easily resolved from the background soil gas compositions with the He/Kr ratio *(Fig. 11)*.

3.3.3 Practical Application

In an attempt to test the potential of the coupling of noble gases with carbon isotopes, we investigated two soil points where high CO_2 concentrations were found at –1 metre, one at a topographical low (42), and one at a topographical
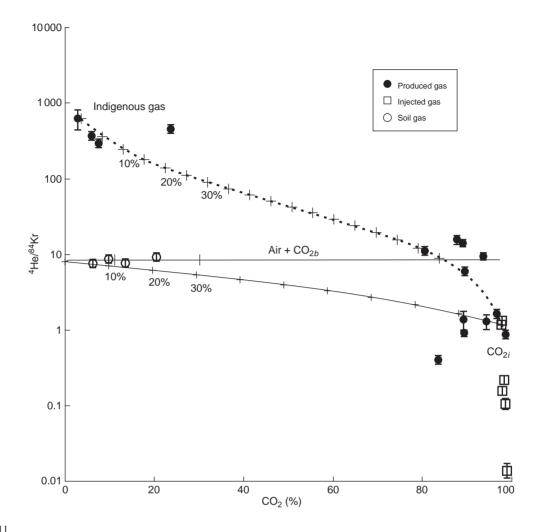
Figure 11

Plot of the ^{4}He over ^{84}Kr ratio *versus* the CO_2 content in injected, reservoir and soil gases. The same mixing curves as in Figure 7 are shown.

high (03) as described earlier *(Fig. 6)*. These points are representative of:

– an apparently normal enrichment with respect to topography (point 42), and;

– an abnormal enrichment with respect to topography (point 03).

At a depth of –5 m, the increase in the CO_2 composition up to 9.8 and 20.5% at these two points, respectively, were favourable for an application of our methodology. The compositions of the noble gases and of δ^{13}C were determined for the –1 m and for the –5 m samples at these two boreholes. There is a clear ambiguity regarding the origin of the CO_2 in these samples only looking at δ^{13}C *(Fig. 8)*. In the He/Kr diagram *(Fig. 11)*, neither is it possible to distinguish the subsurface from the surface CO_2 contributions in the sampled soil gas. On the contrary, the Ar/Kr ratio *(Fig. 10)* makes it

clear that the CO_2 may not be related to a gas leakage from the reservoir to the surface, since the data points are well aligned along the air value, clearly away from the CO_{2i}-air mixing line. Taking the analytical uncertainty of the noble gas analysis into account *(Tab. 4)*, we can discriminate any CO_{2i} from the reservoir in the soil if it represents more than 8% of the soil gas budget. Reducing this uncertainty would drastically improve the detection limit of this method (practically to below 1% CO_2 in soils).

We suggest for point 03, in light of our results, that:

– a biological CO_2 accumulation, and/or;

– a locally enhanced biological productivity;

was induced by either:

• a decrease in permeability due to a horizontal high water saturation in the soil (we indeed observed a one-centimetre

layer of water-saturated soil when drilling the borehole at −2 m) preventing biogenic CO_2 from escaping, or,

- the increased availability of nutrients in this densely developed northern part of the main block (high density of injecting and producing wells). At point 42, the enrichment is found in a topographical low, near a stream, where the bio-geochemical setting is more prone to high soil CO_2 contents.

3.3.4 Applicability of the Method

The methodology presented above needs to be put in the perspective of the various leak scenarios that may be encountered at a geological gas storage site. Such a method may be applied straightforwardly using mixing diagrams, only in the case of a relatively rapid leak of the reservoir fluids to the surface. Indeed, the approach in this paper is simplistic and may not take into account various processes of fluid transport; including diffusion, phase partitioning and fluid-rock interactions, which may all be associated with different leaking pathways. A more realistic and robust application of this method would require the use of flow simulation models from the reservoir to the surface, with a sensitivity analysis of the various parameters that may affect the composition of the fluids throughout migration. However, this first attempt shows how valuable and pertinent the coupling of noble gases with stable isotopes may be to identify the leaks of deeply injected CO_2 at the surface.

CONCLUSIONS

The geochemical case study of the EOR-CO_2 Buracica field has unravelled many areas of technical challenge with respect to the surveillance of geological storage sites. The *in situ* analysis of CO_2 contents in soil has revealed some systematic distribution with topography. The distribution of CO_2 fluxes above the field turned out to be very challenging to interpret without complementary meteorological and petrophysical data. It seems likely that the bulk of the CO_2 found in soils results from *in situ* biological activity in light of its distribution and of its isotopic composition.

At the oil reservoir level, fluids are very heterogeneous in their molecular, isotopic and noble gas compositions. This heterogeneity is a consequence of the EOR-induced sweeping of the petroleum fluids by the injected CO_2, producing a heterogeneous mixing controlled by:

- the production scheme, and;
- the reservoir permeability distribution. The overlapping of the possible CO_2 *versus* $\delta^{13}C$ compositions of the reservoir fluids with the soil gas showed that the isotopic composition of carbon may not be a sufficient tracer of deep fluid leakage at the surface. However, ratios of noble gas isotopes such as $^{40}Ar/^{84}Kr$ were found to be useful

discriminators among the injected gas, the reservoir gas and the atmosphere. With high-precision analytical instruments, leaks would be efficiently identified when producing at least 1% CO_2 in soils at −1 m ge.

A monitoring methodology based on carbon isotopes and noble gases is likely to solve many of the challenges imposed by geological gas storage surveillance, such as reservoir fluid heterogeneities, CO_2 baseline fluctuations and multiplicity of leaking pathways. We suggest further investigation of the coupling of natural geochemical tracers, such as stable isotopes and noble gases, in order to provide the industry with a robust and systematic geochemical monitoring technology. A promising way to do so would be to transpose such tracers into full-scale reservoir simulation models, comparing them with case studies of pilot CCS and EOR projects.

REFERENCES

1 Hermanruda C., Andresena T., Eikena O., Hansena H., Janbua A., Lipparda J., Nordgård Bolåsa H., Simmenesa T.H., Teigea G., Østmo S. (2009) Storage of CO_2 in saline aquifers- lessons learned from 10 years of injection into the Utsira Formation in the Sleipner area, *Energy Procedia* **1**, 1997-2004.

2 Kharaka Y.S., Thordsen J.J., Hovorka S.D., Nance H.S., Cole D.R., Phelps T.J., Knauss K.G. (2009) Potential environmental issues of CO_2 storage in deep saline aquifers: Geochemical results from the Frio-I Brine pilot test, Texas, USA, *Appl. Geochem.* **24**, 1106-1112.

3 White C.M., Strazisar B.R, Granite E.J., Hoffman J.S., Pennline H.W. (2003) Separation and capture of CO_2 from large stationary sources and sequestration in geological formations-coalbeds and deep saline aquifers, *J. Air Waste Manage. Assoc.* **53**, 6, 645-715.

4 Clochard V., Delépine N., Labat K., Ricarte P. (2010) CO_2 plume imaging using 3D pre-stack stratigraphic inversion: A case study on the Sleipner field, *First Break* **28**, 91-96.

5 Dino R., Le Gallo Y. (2009) CCS project in Recôncavo Basin, *Energy Procedia* **1**, 2005-2011.

6 Lino U.R.A (2005) Case history of breaking a paradigm: Improvement of an immiscible gas-injection project in Buracica field by water injection at the Gas/Oil contact, *SPE paper* 94978, pp. 1-8.

7 Prinzhofer A., Vaz Dos Santos Neto E., Battani A. (2010) Coupled use of carbon isotopes and noble gas isotopes in the Potiguar Basin (Brazil): Fluids migration and mantle influence. *Mar. Petrol. Geol.* **27**, 1723-1284.

8 Prinzhofer A., Vega M.A.G., Battani A., Escudero M. (2000) Gas geochemistry of the Macuspana Basin (Mexico): Thermogenic accumulations in sediments impregnated by bacterial gas, *Mar. Petrol. Geol.* **17**, 1029-1040

9 Battani A., Sarda Ph., Prinzhofer A. (2000) Geochemical study of Pakistani natural gas accumulations combining major elements and rare gas tracing, *Earth Planet. Sci. Lett.* **181**, 229-249.

10 Schoell M. (1988) Multiple origins of methane in the Earth, *Chem. Geol.* **71**, 1-10.

11 Gilfillan S.M.V., Sherwood Lollar B., Holland G., Blagburn D., Stevens S., Schoell M., Cassidy M., Ding Z., Zhou Z., Lacrampe-Coulome G., Ballentine C. (2009) Solubility trapping in formation water as dominant CO$_2$ sink in natural gas fields, *Nature* **458**, 614-618.

12 Prinzhofer A., Battani A. (2003) Gas isotope tracing: an important tool for hydrocarbon exploration. Revue de l'IFP, Special Publication for B. Tissot Jubilee, June 2003, *Oil Gas Sci. Technol.* **58**, 2, 299-311.

13 Zhou Z., Ballentine C.J., Kipfer R., Schoell M., Thibodeaux S. (2005) Noble gas tracing of groundwater/coalbed methane interaction in the San Juan Basin, USA, *Geochim. Cosmochim. Acta* **69**, 23, 1, 5413-5428.

14 Sherwood Lollar B., O'Nions R.K., Ballentine C.J (1994) Helium and neon isotope systematics in carbon dioxide-rich and hydrocarbon-rich gas reservoirs, *Geochim. Cosmochim. Acta* **58**, 5279-5290.

15 Prinzhofer A., Rojey A. (2001) Method for quantitative monitoring of a gas injected into a reservoir in particular in a natural environment. Patent Pub. No. WO/2003/010534, International Application No. PCT/FR2002/002643 (2001).

16 Braga J.A.E., Zabalaga J.C., Oliveira J.J, Aguiar G.A., Silva O.B., Mato L.F., Daniel L.M.F., Magnavita L.P., Bruhn C.H.L. (1994) Recôncavo Basin, Brazil: A prolific intracontinental Rift Basin, *AAPG Memoir* **59**, 157-203.

17 Nimz G.J., Hudson G.B. (2005) The use of noble gas isotopes for monitoring leakage of geologically stored CO$_2$, in *Carbon dioxide capture in deep geological formations*, Vol. 2, Thomas and Benson (eds), Elsevier.

18 Jeandel E., Battani A., Sarda P. (2010) Lessons learned from natural and industrial analogues for storage of carbone dioxide, *Int. J. Greenhouse Gas Control* **4**, 890-910.

19 Gaglianone P.C., Trindade L.A.F (1988) Caracterização geoquimica dos oleos da Bacia do Recôncavo, *Geochimica Brasiliensis* **2**, 1, 15-39.

20 De Barros Penteado H.L (1999) Modélisation compositionnelle 2D de la genèse, expulsion et migration du pétrole dans le compartiment sud du bassin de Reconcavo, *PhD Thesis*, Université Pierre et Marie Curie (Paris VI).

21 Famiglietti J.S., Rudnicki J.W., Rodell M. (1998) Variability in surface moisture content along a hillslope transect: Rattlesnake Hill, Texas, *J. Hydrol.* **210**, 259-281.

22 Grieve I.C., Proctor J., Cousins S.A. (1990) Soil variation with altitude on Volcano Barva, Costa Rica, *Catena* **17**, 525-534.

23 Volkoff B., Cerri C.C. (1987) Carbon isotopic fractionation in subtropical Brazilian grassland soils: Comparison with tropical forest soils, *Plant Soil* **102**, 27-31.

24 Rouchon V., Magnier C., Miller D., Bandeira C., Gonçalvez R., Dino R. (2011) The relationship between CO$_2$ flux and gas composition in soils above an EOR-CO$_2$ oil field (Brazil): a guideline for the surveillance of CO$_2$ storage sites, *Energy Procedia* **4**, 3354-3362.

25 Evans W.C., Sorey M.L, Kennedy B.M., Stonestrom D.A., Rogie J.D., Shuster D.L. (2001) High CO$_2$ emissions through porous media: transport mechanisms and implications for flux measurements, *Chem. Geol.* **177**, 15-29.

APPENDIX

High-Resolution Gas Analyses in the Laboratory
A high-resolution gas chromatograph was used to characterise and quantify hydrocarbon and non-hydrocarbon gases collected in glass. The chromatograph, a Varian 3800, is equipped with multiple packed columns, two molecular sieves and a Porapack-N with two TCD and a FID with helium as carrier gas for hydrocarbons C1-C5, CO_2, N_2 and O_2 and nitrogen as a second carrier car for He and H_2 quantification. The precision of the relative content of a gas composition is ±0.1%. The analysis time is 30 minutes.

Stable Carbon Isotopes
The carbon isotope compositions of the sampled CO_2 were analysed from glass Vacutainer® and stainless steel tubes. The $^{13}C/^{12}C$ ratios were measured for C1-C5 hydrocarbons and CO_2 with a MAT Finnigan 253 GC-C-IRMS. The GC operates with a CP-Porabond-Q 25 m × 0.32 mm OD column and helium as carrier gas (gas flow 1.2 mL/min). A gas aliquot is taken through an automated loop sampling (20 μL) in the injector which is heated at 150°C. A split ratio of 135 is applied and enters the column for compound separation, followed by a complete oxidation in a ceramic furnace containing copper oxide, nickel and platinum at 940°C. The CO_2 then proceeds online into the IRMS and carbon isotopic ratios are measured as ratios in delta units with variations expressed in per mil relative to the international PDB standard (Pee Dee Belemnite). Standard deviation and uncertainty in the measurement for the $\delta^{13}C$ for CO_2 is ± 0.3 per mil.

Noble Gas Analyses
The noble gas elementary compositions and the isotopic ratio $^{40}Ar/^{36}Ar$ were determined by a quadripole mass spectrometer (QUADRAR) after treatment of the gas sample through an ultra-high vacuum preparation line. Only samples in stainless steel tubes were analysed in order to guarantee a negligible air noble gas contamination after sampling. The QUADRAR line is able to determine the compositions of He, Ne, ^{40}Ar, ^{36}Ar and Kr. Prior to the analysis, the ultra-high vacuum line is vacuumed to 10^{-9} mbar by three turbomolecular pumps. The inlet part that connects to the sample tube is evacuated under primary vacuum (< 5×10^{-3} mbar). An aliquot of the sample is admitted inside a volume of about 10 cm^3 where its pressure is adjusted and precisely measured by a thermostated capacitance manometer (MKS Baratron®). A 1.2 cm^3 aliquot is then taken out of that volume at a pressure adjusted between 0.1 and 100 mbar (depending on the expected Ar composition). The purification of this aliquot is performed under the action of two titanium foam traps for 30 min. The hot titanium oven is cooled down to ambient temperature and then a precise fraction of the purified gas is admitted into a portion of the line equipped with two activated coal traps and a getter (SAES Getters) GP50 ST707 operating at 3 V. One of the cold traps is maintained at liquid nitrogen temperature (–198°C) in order to trap the heavy gases, Ar and Kr, while He and Ne are analysed by the mass spectrometer before they are evacuated. Then the temperature of the trap is raised to ambient temperature for Ar and Kr

to be desorbed and enter the spectrometer for analysis. The mass spectrometer is a Prisma quadripole QMA/QME200 (Pfeiffer Vacuum) with an open ion source. The analyser allows measurements of compounds with a m/z ratio (mass over charge) from 1 to 100 a.m.u. (atomic mass unit). The mass spectrometer is equipped with two detectors, a Faraday cup and an electron multiplier (SEM), that can be used alternately. The SEM provides a gain of 10 000 compared with the Faraday cup and therefore allows the detection of very small quantities of gas. For each sample, the response of the spectrometer is calibrated by performing systematic analyses of a purified air dose (Calibrated Dose) for which the quantities of He, Ne, Ar and Kr as well as the $^{40}Ar/^{36}Ar$ ratio are controlled weekly by an air standard analysis. The $^{40}Ar/^{36}Ar$ isotopic ratio is calibrated regularly by the tuning of the source. The isobaric interferences of $^{40}Ar^{++}$ and $^{20}Ne^{++}$ are corrected by a calibration made on the background noise and controlled by the measurements of the $^{20}Ne/^{22}Ne$ and $^{20}Ne/^{21}Ne$ ratios. Interference of CO_2 on mass 44 with ^{22}Ne is always negligible. A blank for the entire line is measured every week and does not exceed 1 ± 2% of the signal of a Calibrated Dose (DC). The mean blank is subtracted to the signal of the sample and its standard deviation is integrated to the uncertainty of the sample analysis. The control over the introduction pressure of the sample allows a very low detection limit, implying no limitation when analysing natural samples. Global relative uncertainty (at 1σ) for quantification of noble gases with this method is: He: ± 10%; Ne: ± 20%; Ar: ± 5%; Kr: ± 8%, and for quantification of the ratio $^{40}Ar/^{36}Ar$ ± 1%.

Helium isotopic ratios and contents were determined by the means of a high-resolution magnetic sector mass spectrometer Micromass 5400. Prior to analysis, the gases are purified and separated in a line under ultra-high vacuum as described for QUADRAR. Thus, helium is introduced into the mass spectrometer under an optimal partial pressure, allowing very accurate and sensitive quantification. The mass spectrometer is equipped with a modified Nier-type electron impact source (Bright). A permanent magnet in the ionisation zone allows a better yield for the source. The latter is adjusted in order to obtain an optimal signal for helium. The GV 5400 comprises a Faraday cup and an electron multiplier (Balzers SEM 217). These collectors are used alternately for the $^3He/^4He$ ratio analysis. The most abundant isotope (^4He) is measured on the Faraday cup, whereas ^3He is measured by the electron multiplier. A resolution of 600 is obtained on the electron multiplier and is also necessary and sufficient for a good separation of ^3He from the HD background in the high-vacuum line. Twenty successive measurements are performed for each isotope. A statistical regression is done in order to determine the intensity of the signal at the time of gas introduction into the source. Calibration of the mass spectrometer is similar to that described earlier for QUADRAR. The blank is measured every week and represents 0.1% of the helium signal in the sample or the standard. The overall uncertainty on the quantification of ^4He is ± 4%. For the $^3He/^4He$ ratio it is ± 2%.